

2nd International Conference on System-Integrated Intelligence: Challenges for Product and Production Engineering

## Component integrated sensors: Deposition of thin insulation layers on functional surfaces

D. Klaas<sup>a\*</sup>, P. Taptimthong<sup>a</sup>, L. Jogschies<sup>a</sup>, L. Rissing<sup>a</sup>

<sup>a</sup>*Institute for Micro Production Technology, Centre for Production Technology, Leibniz Universität Hannover, An der Universitaet 2, 30823 Garbsen, Germany*

---

### Abstract

To guarantee the deposition of sensors on functional surfaces, a reliable thin insulation layer is required. Within this paper, the results of the investigation of a capable insulation layer are presented. Challenges occurring during the manufacturing process will be discussed. A focus is set on parameters that influence the breakdown field strength. The influence of the surface roughness on the quality of the produced layers will be discussed as well. Differences between layers deposited on stainless steel and on aluminium will be mentioned.

© 2014 Published by Elsevier Ltd. This is an open access article under the CC BY-NC-ND license (<http://creativecommons.org/licenses/by-nc-nd/3.0/>).

Peer-review under responsibility of the Organizing Committee of SysInt 2014.

*Keywords:* Sensor; Insulation layer; Gentelligent; Dialuminiumtrioxid; Al<sub>2</sub>O<sub>3</sub>; Collaborative Research Centre 653

---

### 1. Introduction and Motivation

Within the Collaborative Research Center 653 genetic and intelligent components are developed which are able to store information such as the mechanical stress or their lifetime intrinsically. Furthermore, those “gentelligent”<sup>TM</sup> components are able to monitor their own conditions autonomously and call for inspection if essential [1].

Various sensors were developed previously to capture manifold information of the component like the strain, the

---

\* Corresponding author. Tel.: +49-511-762-18028; fax: +49-511-762-2867.

E-mail address: [klaas@impt.uni-hannover.de](mailto:klaas@impt.uni-hannover.de)

applied force or the temperature. In the first approach, the sensors were manufactured on a thin silicon substrate that was later replaced by a thin polyimide film to increase the level of system integration [2]. The development of the polyimide-based sensors required the investigation of various manufacturing technologies to overcome challenges like warping of the sensors caused by polyimide film stress, adhesion of the deposited layers and homogeneity of the sensors. To avoid warping and to mechanically stabilise the structure of the sensor, polyimide was deposited onto silicon wafers, cured and patterned with several functional deposition layers to form the final sensor [3]. Later on, a grid like silicon structure has been manufactured using backside deep reactive ion beam etching. The silicon structure serves as a frame. It spans the film based batch-manufactured sensors and allows an easy separation by using a stamping tool.

However, an adhesive layer is required to attach the sensors onto surfaces of components. This inevitably reduces attainable sensitivity. To reduce the influence of those films on the measurands, a new sputtering system and manufacturing technology will be developed that enables a direct deposition of the sensors on a functional surface. As most components within machines, devices and facilities are made of aluminum alloys or stainless steel, AlMg3 (3.3535) and stainless steel (1.4305) are used as reference substrates for the deposition. As both materials are electrically conductive, it is essential to investigate thin insulation layers that can be directly deposited onto the surfaces of the components.

High purity 4N-aluminium oxide ( $\text{Al}_2\text{O}_3$ ) is used as the material for the insulation layers. The used  $\text{Al}_2\text{O}_3$  offers advantages such as a good electrically insulating property with a breakdown field strength of up to 30 V/ $\mu\text{m}$ , a high mechanical wear-resistance and a high chemical resistance. Moreover, it is stable over a wide temperature range of up to approximately 2000 °C [4].

To measure the insulation properties of the produced  $\text{Al}_2\text{O}_3$  layers, a capacitor-like layer composition has been realised. In the first step, the analysed substrates have been covered with a sputtered 500 nm thick chromium layer, forming the lower contact pad. Afterwards the insulation layers have been produced with different layer thickness varying between 500 nm and 3,000 nm. Finally, a shadow mask has been used to structure the varied upper contact pads consisting of a 500 nm thick chromium layer.

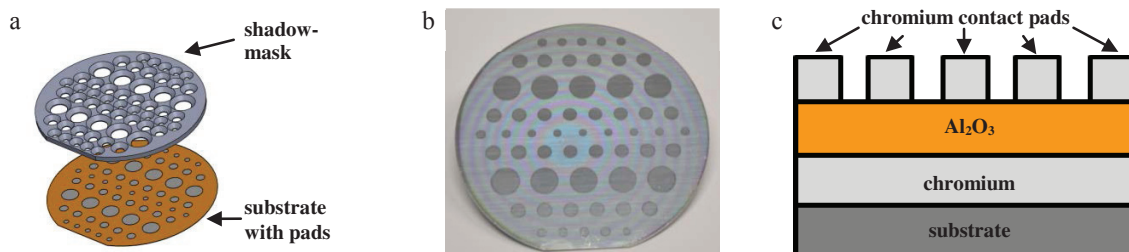


Fig. 1. (a) Schematic of the structuring process by using a shadow mask; (b) Picture of a coated and structured substrate; (c) Sectional view of the layer composition.

The structured circular contact pads were arranged in an equidistant, repetitive order with diameters of 3 mm, 5 mm and 10 mm to allow the investigation of the uniformity of the deposition and the influence of the size of the contact pads and their position on the insulation capability. The radiofrequency sputtering (RF-sputtering) has been carried out by using a Senvac Z550 sputter system with two “dressler CESAR” RF-powering generators. The used targets had a diameter of 6,5 inch (165,1 mm) and have been used without a magnetron. Substrates have been not heated and at a temperature of 200°C maximum during the sputtering process. The deposition rate has been at about 8 nm/ min at 400 W RF-power under 50 sccm argon flow rate.

The paper consists of four sections. The following section 2 describes the setup for measuring the electrical resistance of the insulation layers and the breakdown voltage. Section 3 presents the improvements made to increase the insulation capability. A focus is set on the influence of two parameters, the surface roughness and the base pressure, on the insulation layer quality. At the end of section 3, the results are discussed. Section 4 summarises the paper and gives a brief perspective for future investigations.

Former work in the field of insulation layers has been done by various research groups. Wallin [5] describes the growth of thin  $\text{Al}_2\text{O}_3$  layers deposited by reactive sputtering, investigating the dependence of the layer thickness from the substrate temperature and gas pressure. Measurements on the insulation layers were not carried out. A design of experiments to investigate the correlation between various sputter parameters, such as the substrate temperature, sputtering power, produced layer thickness and its insulation quality was carried out by Schmaljohann et al. [6]. The surface roughness of the used steel surface was reduced significantly by polishing. As it is complicated and time-consuming to polish the surface of technical components to such a low mean surface roughness, the developed technique cannot be used for real technical surfaces. Similar work was done by Li et al., who investigated layers sputtered with a radiofrequency-technology [7] and Cremer et al. [8], who used radiofrequency, direct current and pulsed sputtering technologies. However, very few work was carried out for stainless steel (1.4301) and AlMg3 (3.3535) as surface substrates.

## 2. Measurements of the Insulation Layers

To determine the insulation capability of the  $\text{Al}_2\text{O}_3$  layers, their electrical resistance and breakdown voltage have been measured. To allow a reproducible measurement, a testing measurement setup has been designed (figure 2). The bottom contact pad on the substrate is contacted with a clamp while the upper contact pads are contacted by using an easily to position measurement tip. The results indicate that the contact position of the tip on the pad has no influence on the measured electrical resistance and that the weight of the tip produces a sufficient contact pressure for repetitious measurements. To precisely define the measurement technique, the tip has been placed in the middle of each contact pad.

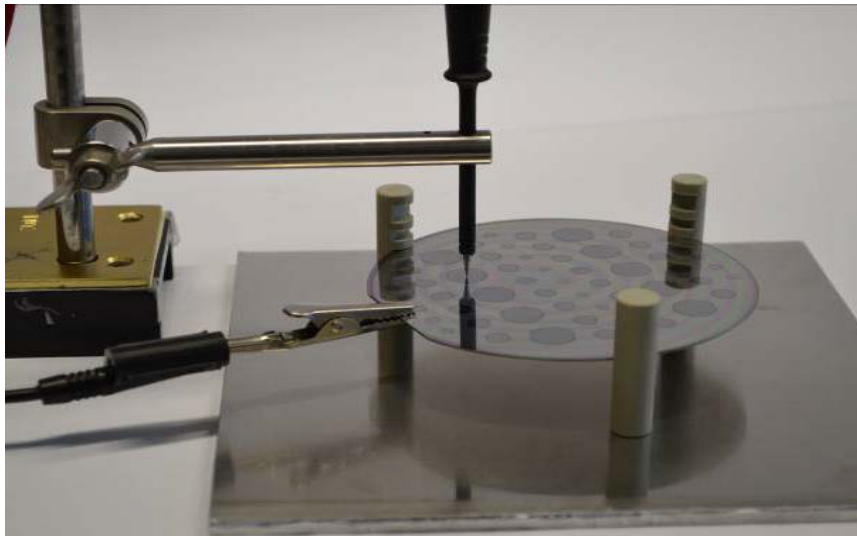


Fig. 2. Picture of the testing setup with the measuring tip placed in the middle of a contact pad.

### 2.1. Measuring of the Electrical Resistance and the Breakdown Voltage

The electrical resistance of the insulation layer between the two contact pads of the capacitor is measured with the measuring tip using an Agilent 34410 A, a digital multimeter. The breakdown voltage has been measured with a Fischer Elektronik Tera-Ohmmeter TO-3 by increasing the insulation test voltage stepwise by 1 V and measuring the current flowing through the insulation layer. A breakdown is defined at an electrical resistance smaller than 1 G $\Omega$ . As soon as the limitation current is reached, the measurement stops automatically. The average values of the breakdown voltage for the insulation layers deposited on aluminum and stainless steel substrates are illustrated in table 1. Those values represent the test results for the first charge of produced layers.

Table 1. Maximum achieved breakdown voltage of Al<sub>2</sub>O<sub>3</sub> insulation layers deposited on AlMg3 (3.3535) and stainless steel (1.4305) substrates at the beginning of the research without any process optimisation.

substrate material	Al <sub>2</sub> O <sub>3</sub> layer thickness	breakdown voltage	breakdown field strength
AlMg3 (3.3535)	1,000 nm	2.1 V	2.10 V/ μm
AlMg3 (3.3535)	3,000 nm	4.3 V	1.43 V/ μm
stainless steel (1.4305)	3,000 nm	3.6 V	1.20 V/ μm
stainless steel (1.4305) (machined surface)	3,000 nm	5.4 V	1.80 V/ μm

## 2.2. Discussion of the Results

The electrical resistance measurement indicates that the insulation layer resistance is depending on the contact pad size and the position of the pad on the wafer. The greater the contact pad diameter, the lower the electrical resistance of the insulation layer. Investigations proved that the insulation layer thickness is not equal over the substrate but radially alternating. Further investigations revealed that the contact pad size has an influence on the electrical resistance and the breakdown voltage. This is a result of the higher probability of layer defects caused by deposition or surface damages (described in section 3). The larger the contact pad size is, the higher the probability of defects.

With respect to the material of the coated substrates, the maximum achieved breakdown voltage is at approximately 4.3 V for AlMg3 and at 3.6 V for stainless steel. The layer thickness of Al<sub>2</sub>O<sub>3</sub> was 3,000 nm for both materials (table 1). To ensure sufficient insulation capability, the breakdown voltage has to be three times larger than the 5 V operating voltage of the sensors. According to the measured values and in conjunction with the theoretically possible breakdown field strength of 30 V/ μm, the produced insulation layer quality is inadequate and has to be improved.

## 3. Improvement of the Insulation Capability

One of the most interesting observations during the measurements of the breakdown voltage is an effect of small craters appearing on the surface of the upper contact pads a few seconds before the breakdown occurs (figure 3). By increasing the insulation test voltage, the diameter of the craters grows. The appearance and growth of the craters is independent of the position of the measurement tip on the contact pads and occurs simultaneously to the decreasing of the electrical resistance.

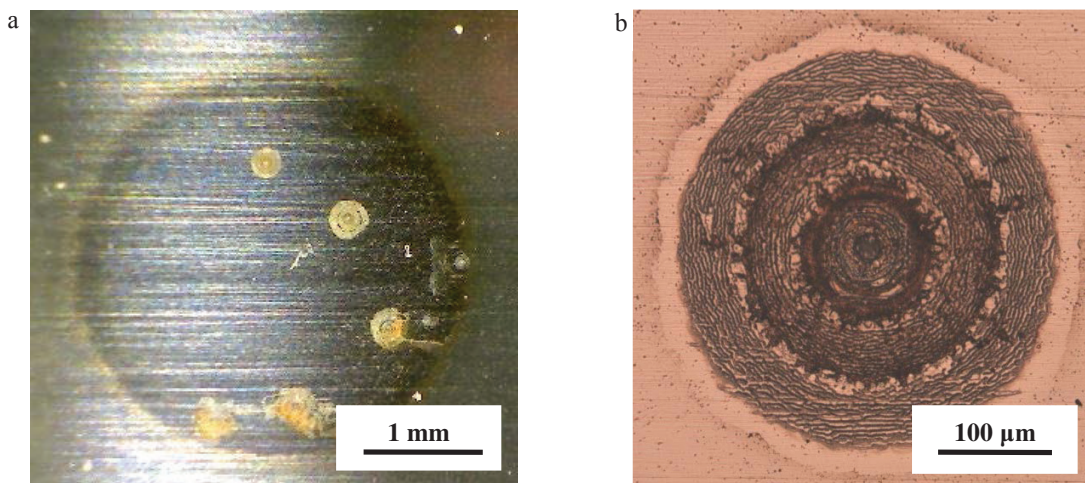


Fig. 3. (a) Optical microscope image of a 3 mm contact pad with craters on the surface as a result of the breakdowns; (b) Micrograph of a crater.

By measuring within a dark environment, small sparks between the lower and upper contact pad are observed at the moment of breakdown. It has to be mentioned, that even on a single contact pad plenty of breakdowns are observed, each reducing the measured electrical resistance of the insulation layer.

### 3.1. Research on the Breakdowns

To identify reasons for the craters and the breakdowns, investigations on the surface topology of uncoated AlMg3 and stainless steel substrates are carried out. As the scanning electron microscope (SEM) picture shows, the planar surfaces of the substrates inherently possess small particles randomly distributed. These particles increase the surface roughness significantly (figure 4). They have a height of up to 4  $\mu\text{m}$  and a width of up to 16  $\mu\text{m}$ .

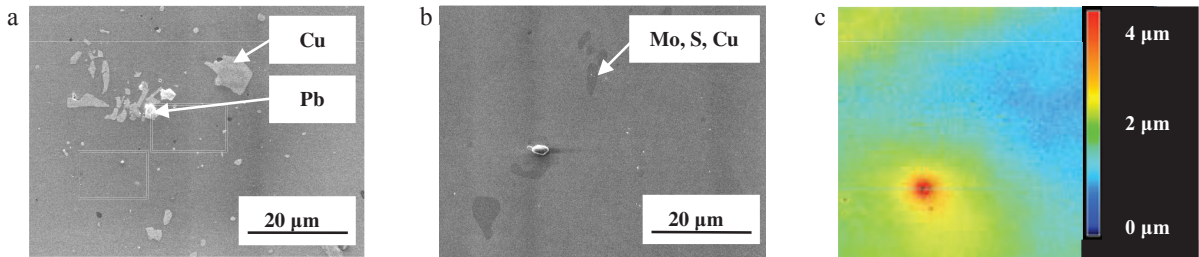


Fig. 4. (a) Scanning electron microscope (SEM) picture of the AlMg3 (3.3535) surface and information about the identified particles. Identification was done by using energy dispersive X-ray spectroscopy (EDX); (b) Scanning electron microscope picture of the stainless steel surface and information about the identified particles; (c) Confocal laser scanning microscope image of the surface topography of an uncoated stainless steel (1.4305) substrate embossing the surface [10].

By using the energy dispersive X-ray spectroscopy (EDX), the particles were analysed. It can be seen, that all detected particles are additives of the AlMg3 and stainless steel alloys (table 2 and table 3). The particles are used as e.g. chip breakers within the different materials to allow an easier machining of the material or to improve the mechanical behaviour.

Table 2. Theoretical alloy composition of AlMg3 (3.3535) [10]

alloy component	chemical symbol	concentration
Aluminium	Al	94.95%
Magnesium	Mg	3 %
Manganese	Mn	0.5 %
Iron	Fe	0.4 %
Silicon	Si	0.4 %
Chromium	Cr	0.3 %
Tin	Zn	0.2 %
Titan	Ti	0.15 %
Copper	Cu	0.1 %

Table 3. Theoretical alloy composition of stainless steel (1.4305) [11]

alloy component	chemical symbol	concentration
Iron	Fe	54.08-62.78 %
Chromium	Cr	16-19 %
Nickel	Ni	5-10 %
Manganese	Mn	6.5 %
Molybdenum	Mo	6.5 %
Copper	Cu	1.75-2.25 %
Silicon	Si	1 %
Sulphur	S	0.15-0.35 %
Phosphorus	P	0.2 %
Carbon	C	0.12 %

The high emboss caused by the particles reflect the high values of the surface roughness. Whereas the values of the arithmetical mean roughness  $R_a$  of AlMg3 and stainless steel are relatively low; the chip breakers have a high influence on the average surface roughness  $R_z$  (table 4). The influence of the chip breakers can be described as follows. Due to their height, they reduce the effective thickness of the insulation layer. Researched showed that the breakers are not completely covered with the deposited  $\text{Al}_2\text{O}_3$  insulation layer. This results in a lower breakdown voltage.

Table 4. Surface roughness of the uncoated substrates used at the beginning of the research.

substrate material	arithmetical mean roughness $R_a$	average surface roughness $R_z$
AlMg3 (3.3535)	450 nm	16,550 nm
stainless steel (1.4305)	8,170 nm	88,040 nm
stainless steel (1.4305) (machined surface)	429 nm	18,009 nm

### 3.2. Influence of the Base Pressure on the Insulation Capability

The breakdowns occur not only due to the chip breakers but also as a result of defects, e.g. pin holes, and inhomogeneous insulation layers, both caused by the sputtering process. To minimise the influence of the chip breakers, further investigations to improve the insulation capability are carried out on silicon wafers. Those wafers are planar and have a surface roughness of just  $R_{a,Si} = 0.2$  nm and an average surface roughness of just  $R_{z,Si} = 1$  nm.

Research on topology using a Hysitron Nanoindenter TI-900 indicates that the base pressure within the sputtering chamber before the start of the sputtering process has a significant influence on the insulation capability (figure 5). At a low pressure of  $p = 0.12$  mPa, the deposited  $Al_2O_3$  layers are more homogeneous and have very low surface roughness with little surface peaks of up to 4 nm maximum. Whereas at a higher pressure of  $p = 0.9$  mPa the produced  $Al_2O_3$  layers are clearly rougher and show surface peaks of up to 118 nm [9].

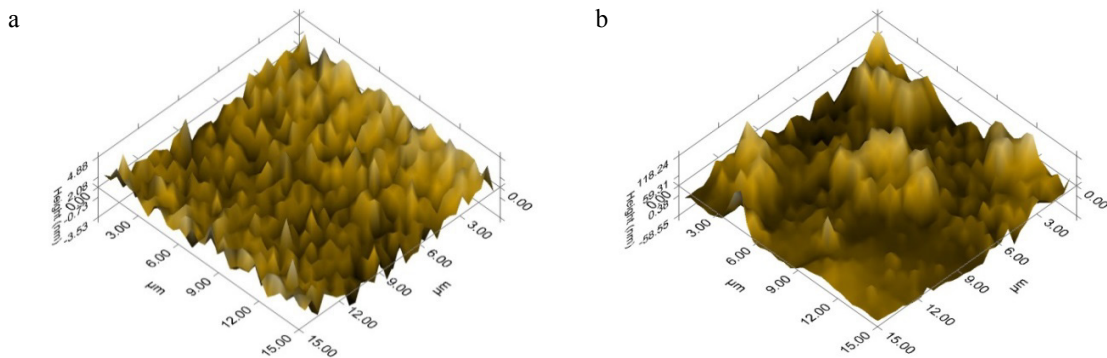


Fig. 5. Influence of the pressure on the insulation layer: (a) Topological image of the surface profile of an  $Al_2O_3$  layer coated on a silicon wafer at a pressure of 0.12 mPa; (b) Topological image of the surface profile of a  $Al_2O_3$  layer coated on a silicon wafer at a pressure of 0.9 mPa.

The influence of the pressure is a result of the longer mean free path of the gas ions. This results in a higher kinetic energy of the sputtered  $Al_2O_3$  molecules. The high energy  $Al_2O_3$  molecules are densely packed onto the substrates leading to a thinner and improved insulation layer. Furthermore, the higher kinetic energy of the molecules and the resulting higher impact will lead to a better layer adhesion on the substrates. This will have a positive influence on the sensitivity of the sensor, as the deformation of the insulation layer will be close to the reality of the deformation of the component on which it is applied.

### 3.3. Discussion on the Results of the Improved Layers

The improved insulation layers are manufactured on silicon, AlMg3 and stainless steel with the reduced base pressure. Furthermore, high quality polished AlMg3 and stainless steel substrates have been employed. The measurement results are shown in table 5.

The insulation voltage for the layers produced on silicon is increased up to 23.1 V for 2,000 nm thick layers, that equals a breakdown field strength of 11.55 V/ $\mu$ m. Nevertheless, the breakdown voltage and the breakdown field strength does not increase linearly with the thickness of the insulation layer (table 5). While the thickness of the

insulation layer is doubled, the breakdown voltage for the silicon substrate is increased by just 34 %. Hence, the breakdown field strength is reduced from 17.30 V/ $\mu\text{m}$  for 1000 nm thick insulation layers to just 11.55 V/ $\mu\text{m}$  for 2,000 nm insulation layers.

The reduction of the surface roughness by a high quality polishing decreased the average surface roughness for AlMg3 by 14 % and for stainless steel by up to 192 %. However, the average surface roughness is still too high compared to the arithmetical mean roughness. Thus, it has high influence on the insulation capability. The results of the insulation layers deposited on AlMg3 and stainless steel is lower compared to silicon substrates with a breakdown voltage of just 15.1 V for AlMg3 and 11.8 V to 17.4 V for stainless steel. Hence, the required voltage security factor of more than three is reached for AlMg3 and machined stainless steel. For unmachined stainless steel the security factor is just 2.36.

Table 5. Breakdown voltage of the optimised insulation layers deposited on silicon wafers, AlMg3 (3.3535) and stainless steel (1.4305) and the average surface roughness achieved by high quality polishing of the surface.

substrate material	Al <sub>2</sub> O <sub>3</sub> layer thickness	breakdown voltage	breakdown field strength	arithmetical mean roughness R <sub>a</sub>	average surface roughness R <sub>z</sub>
Silicon	500 nm	8.1 V	16.20 V/ $\mu\text{m}$	< 0.2 nm	< 1 nm
Silicon	1,000 nm	17.3 V	17.30 V/ $\mu\text{m}$	< 0.2 nm	< 1 nm
Silicon	2,000 nm	23.1 V	11.55 V/ $\mu\text{m}$	< 0.2 nm	< 1 nm
AlMg3 (3.3535)	3,000 nm	15.1 V	5.03 V/ $\mu\text{m}$	210 nm	14,073 nm
stainless steel (1.4305)	3,000 nm	11.8 V	3.93 V/ $\mu\text{m}$	683 nm	30,080 nm
stainless steel (1.4305) (machined surface)	3,000 nm	17.4 V	5.80 V/ $\mu\text{m}$	320 nm	15,800 nm

#### 4. Summary of the Results and Perspective

The improvement of insulation layers deposited on silicon wafers, AlMg3 (3.3535) and stainless steel (1.4305) substrates have been investigated. The surface roughness and especially the pressure within the sputtering chamber have a significant influence on the insulation layer breakdown voltage and quality. The current insulation thickness of 3,000 nm is a satisfying reduction of the actual 15,000 nm thick layer used as a flexible substrate for the polyimide-based sensors [2, 12]. Furthermore, the theoretical breakdown field strength of 30 V/ $\mu\text{m}$  allows an optimisation by thinning the Al<sub>2</sub>O<sub>3</sub> insulation layer. By reducing the thickness of the insulation layer, the lowest thickness possible, with respect to an adequate and fail safe insulation layer, needs to be investigated.

Moreover, the planarisation technology offers good perspectives to reduce the surface roughness significantly and should be enhanced. Furthermore, research on permanent strength of the deposited layers and the surface adhesion is needed. According to pre-examinations, the focus should be set on the sputtering parameters such as the sputtering power, the bias voltage, substrate temperature and on the distance between the target and substrate surface.

#### Acknowledgements

This work was funded by the German Research Foundation as part of the Collaborative Research Centre 653: “Gentelligent Components in their Lifecycle” within the sub-project S1 “Modular, Multifunctional Micro Sensors” at the Institute for Micro Production Technology, Centre for Production Technology, Leibniz University of Hanover, Germany.

#### References

- [1] SFB 653. The Collaborative Research Centre “Gentelligent Components in their Lifecycle”, Centre for Production Technology, Leibniz Universität Hannover, Germany; <http://www.sfb653.uni-hannover.de/en-us/Pages/Der-SFB.aspx> (4th Nov. 2013).
- [2] Griesbach T, Wurz MC, Rissing L. Development and Fabrication of Modular Micro Sensors on Flexible Polymer Foils. Proceedings of the 1th Joint International Symposium System-Integrated Intelligence 2012: New Challenges for Product and Production Engineering 2012.

- [3] SFB 653. Subproject S1: Modular, Multifunctional Micro Sensors, Centre for Production Technology, Leibniz University of Hanover, Germany; <http://www.sfb653.uni-hannover.de/en-us/Pages/Teilprojekt-S1.aspx>, (5th Nov. 2013).
- [4] Sindlhauser Materials GmbH, Aluminium oxide sputtering target (safety data sheet). 26th June 2013, Kempten, Germany.
- [5] Wallin E. Alumina Thin Film Growth: Experiments and Modeling. Licentiate Thesis, Linköping University 2007.
- [6] Schmaljohann F, Hagedorn D, Löffler F. Systematic evaluation of thin electrically insulating layers on common engineering material. 13th International Conference on Plasma Surface Engineering, Proceedings 2012.
- [7] Li Q, Yu Y-H, Bhatia C, Marks LD, Lee SC, Chunga YW. Low-temperature magnetron sputter-deposition, hardness, and electrical resistivity of amorphous and crystalline alumina thin films. *Journal of Vacuum Science & Technology A* 2000;18(5):2333-2338.
- [8] Cremer R, Witthaut M, Neuschütz D, Erkens G, Leyendecker T, Feldhege M. Comparative characterization of alumina coatings deposited by RF, DC and pulsed reactive magnetron sputtering. *Surface and Coating Technology* 1999;120-121:213-218.
- [9] Miethke S. Fertigung und Charakterisierung von gesputterten Mikrostrukturen mit Schattenmasken. Bachelor-Thesis, Leibniz University of Hanover 2012
- [10] Schmolz+Bickenbach. AlMg3 (3.3535) (data sheet). Düsseldorf; 2011. <http://www.schmolz-bickenbach.de/fileadmin/files/schmolz-bickenbach.de/documents/Datenblaetter/5754.pdf>Sensors, (12th Feb. 2014).
- [11] Erich Uhe GmbH. 1.4305 Werkstoffdatenblatt (gem. Stahlschlüssel). Hemmingen. <http://www.uhe.de/uploads/media/1.4305.pdf>, (11th Feb. 2014).
- [12] Griesbach T, Wurz MC, Rissing L. Application of Sacrificial Layers for the Modular Micro Sensor Fabrication on an Flexible Polymer Substrate. *Sensors and Test Congress and Exposition, Proceedings* 2011.